Wollaston prism-like devices based on blazed dielectric subwavelength gratings

Riad Haïdar, Grégory Vincent, Nicolas Guérineau, Stéphane Collin*, Sabrina Velghe, Jérôme Primot

Office National d'Etudes et de Recherches Aérospatiales, Chemin de la Hunière, F-91761 Palaiseau cedex
** Laboratoire de Photonique et des Nanostructures, Route de Nozay, F-91460 Marcoussis*
haidar@onera.fr

Abstract: A Wollaston prism-like binary dielectric grating is presented and analyzed. It behaves like a transmission grating, differentially and symmetrically blazed for the two crossed polarization states, TE and TM. The phase profile is obtained by means of subwavelength structures etched in a high optical index isotropic dielectric medium (gallium arsenide, for instance). The performance of the device is illustrated by numerical examples and sketched in terms of spectral bandwidth and of extinction ratio. Some practical issues related to the fabrication are discussed.

OCIS Codes: (050.1970) Diffractive optics ; (230.1360) Beam splitters; (260.5430) Polarization.

References and links

1. E. Noponen, A. Vasara, J. Turunen, J. Michael Miller, and M. R. Taghizadeh, "Synthetic diffractive optics in the resonance domain," J. Opt. Soc. Am. A **9**, 1206-1213 (1992).
2. S. Astilean, Ph. Lalanne, P. Chavel, E. Cambril and H. Launois, "High-efficiency subwavelength diffractive element patterned in a high-refractive-index material for 633 nm," Opt. Lett. **23**, 552-554 (1998).
3. L. Pajewski, R. Borghi, G. Schettini, F. Frezza, and M. Santarsiero, "Design of a Binary Grating with Subwavelength Features that Acts as a Polarizing Beam Splitter,**"** Appl. Opt. **40**, 5898–5905 (2001).
4. G. Bouchitté, and R. Petit, *Electromagnetics*, 5, 17-36 (1985).
5. D. L. Brundrett, E. N. Glytsis, and Th. K. Gaylord, "Homogeneous-layer models for high-spatial-frequency dielectric surface-relief gratings: conical diffraction and antireflection designs," Appl. Opt. **33**, 2695-2706 (1994).
6. L.H. Cescato, E. Gluch, and N. Streibl, "Holographic quarterwave plates," Appl. Opt. **29**, 3286-3290 (1990).
7. H. Kikuta, Y. Ohira, and K. Iwata, "Achromatic quarter-wave plates using the dispersion of form birefringence," Appl. Opt. **36**, 1566–1572 (1997).
8. G. Nordin and P. Deguzman, "Broadband form birefringent quarter-wave plate for the mid-infrared wavelength region," Opt. Express **5**, 163–168 (1999), http://www.opticsexpress.org/abstract.cfm?URI=OPEX-5-8-163
9. K. Knop, "Reflection grating polarizer for the infrared," Opt. Commun. **26**, 281–283 (1978)
10. U. Levy, C. H. Tsai, L. Pang, and Y. Fainman, "Engineering space-variant inhomogeneous media for polarization contro,l" Opt. Lett. **29**, 1718–1720 (2004).
11. W. Stork, N. Streibl, H. Haidner, and P. Kipfer, "Artificial distributed-index media fabricated by zero-order gratings," Opt. Lett. **16**, 1921-1923 (1991)
12. W. M. Farn, "Binary gratings with increased efficiency," Appl. Opt. **31**, 4453-4458 (1992).
13. S. M. Rytov, "Electromagnetic properties of a finely stratified medium," Sov. Phys. JETP **2**, 466-475 (1956).
14. Ph. Lalanne and D. Lemercier-Lalanne, "On the effective medium theory of subwavelength periodic structures," J. of Mod. Opt. **43**, 2063-2086 (1996).
15. J. M. Bell, G.H. Derrick, and R.C. McPhedran, "Diffraction gratings in the quasi-static limit," Optica Acta **29**, 1475 (1982).
16. R. Brauer, and A. Bryngdahl, "Design of antireflection gratings with approximate and rigorous methods," Appl. Opt. **33**, 7875-7882 (1994).
17. D.A. Pommet, M.G. Moharam and E.B. Grann, "Limits of scalar diffraction theory for diffractive phase elements," J. Opt. Soc. Am. A **11**, 1827-1834 (1994).
18. Ph. Lalanne and D. Lemercier-Lalanne, "Depth dependence of the effective properties of subwavelength gratings," J. Opt. Soc. Am. A **14**, 450-458 (1997).

#9238 - $15.00 USD Received 25 October 2005; revised 18 November 2005; accepted 21 November 2005

19. I. Richter, P.C. Sun, F. Xu and Y. Fainman, "Design considerations of form birefringent microstructures," Appl. Opt. **34**, 2421-2429 (1995).
20. S. Adachi, "GaAs, AlAs, and AlxGa1–xAs Material parameters for use in research and device applications," J. Appl. Phys. **58**, R1-R29 (1985).
21. H. Moussa, R. Daneau, C. Mériadec, L. Manin, I. Sagnes, and R. Raj, "Deep in situ dry-etch monitoring of III-V multilayer structures using laser reflectometry and reflectivity modeling," J. Vac. Sci. Technol. A **20**, 748-753 (2002).
22. W. J. Zubrzycki, G. A. Vawter, and J. R. Wendt, "High-aspect-ratio nanophotonic components fabricated by Cl_2 reactive ion beam etching," J. Vac. Sci. Technol. B **17**, 2740–2744 (1999).
23. M. V. Kotlyar, L. O'Faolain, R. Wilson, and T. F. Krauss, "High-aspect-ratio chemically assisted ion-beam etching for photonic crystals using a high beam voltage-current ratio," J. Vac. Sci. Technol. B **22**, 1788–1791 (2004).
24. H. Lajunen, J. Turunen and J. Tervo, "Design of polarization gratings for broadband illumination," Opt. Express **13**, 3055-3067 (2005), http://www.opticsexpress.org/abstract.cfm?URI=OPEX-13-8-3055

1. Introduction

Polarizing beam splitters (PBS) are important devices for optical systems, should they be used for information-processing applications, for routing devices, or for conventional imaging systems. A PBS splits an incident light beam into two crossed polarized beams. It should present good extinction ratios and broad wavelength range. Wollaston, Taylor or Rochon prisms make use of natural birefringence of some crystals, such as quartz for the visible range, or MgF_2 for the infrared. Other PBS are based on multilayer dielectric coatings, or on the polarization-selective properties of diffractive optical elements.

This paper deals with a new class of such diffractive binary PBS. To date, one-dimensional subwavelength binary PBS only acted on one polarization, being non-diffractive for the other polarization[1,2], or acted on the differential phase shift of one polarization relative to the other[3]. The device presented here acts as a Wollaston-prism, i.e. it symmetrically diffracts the two polarization states, that is in two directions that are symmetrical versus the grating normal. We thus call it a Wollaston prism-like device (WPD). This particular diffraction pattern ensures an equal optical path for both polarizations, thus allowing interference applications.

The WPD is based on subwavelength dielectric one-dimensional structures. These structures are designed for use under normal incidence in air. Then, as is well-known, a diffraction grating with a structure dimension smaller than the wavelength of light does not generate real diffracted orders, except for the zeroth order. From a macroscopic point of view, these structures behave as homogeneous uniaxial anisotropic media, with a modulated optical index for both the ordinary and extraordinary waves[4]. They have suggested interesting applications, such as anti-reflection coatings, quarter-wave plates or polarizers[5-10]. The principle of the WPD is that of a differentially blazed grating : each period of the grating is itself divided in two sub-periods, each sub-period being nanostructured so that it is specially blazed for one polarization (TE or TM, TE being the one for which vector **E** is parallel to the grating slits). So the WPD could be understood as the lateral superposition of two blazed gratings. Though various geometries can be imagined, we will focus on the geometry of Fig. 1.

#9238 - $15.00 USD Received 25 October 2005; revised 18 November 2005; accepted 21 November 2005

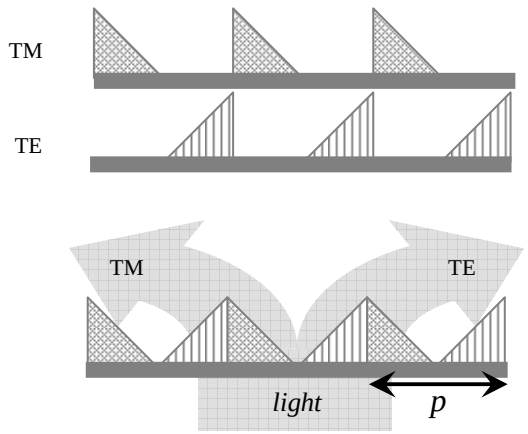

Fig. 1. Schematic diagram of a Wollaston Prism-like Device (WPD), using a variation of phaseshift between 0 and 2π.

A blazed grating diffracts light essentially in a given order. For this, it needs to realize the linear variation of the phase φ of the diffracted light from $2\pi(l-1)$ to $2\pi l$ (l an integer) within one single sub-period, and this for each polarization state. It is possible to code a phase modulation, $\varphi(x)=ne$, by two optically equivalent means[11,12]: either a variation of the structure depth $e(x)$ for a given n as is the case for "echelette" gratings, or symmetrically a variation of its optical index $n(x)$ for a given e. As a differential behaviour of the grating for the two polarization states is wanted, the only possible solution is to act on the modulation of the index n, which indeed can be polarization-dependent. This is obtained here through subwavelength structures, as is shown on Fig. 2.

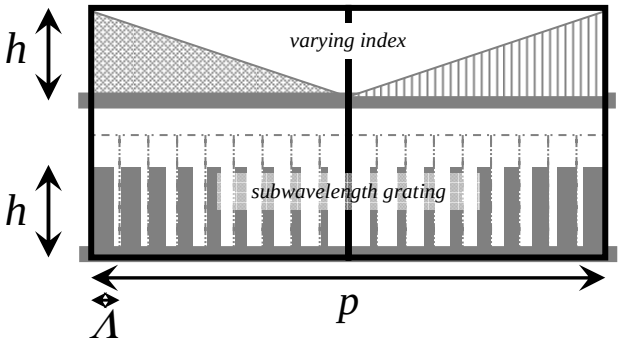

Fig. 2. Coding a linearly-varying effective index (or similarly, a linearly-varying phaseshift) with subwavelength gratings of varying fill-factor, for a given polarization state.

In Section 2, we describe the approximations and the method used to determine the effective index of the subwavelength structures. In Section 3, we sketch one possible WPG structure on gallium arsenide (GaAs), and compare it to the state-of-the-art possibilities in terms of etching techniques. In Section 4, we evaluate the diffraction efficiency of the WPG structure. A spectral study is also presented, and shows that the WPG are spectrally broadband.

#9238 - $15.00 USD Received 25 October 2005; revised 18 November 2005; accepted 21 November 2005

2. Effective index computation

We consider the long-wavelength regime, which may be defined as follows: the typical dimension of the subwavelength structures is very small as compared to the wavelength. In this regime, the effective medium theory (EMT) is an adequate tool to calculate the effective index of a one-dimensional structure. A closed-form EMT solution for one-dimensional periodic lamellar structures composed of two homogeneous materials was first derived by Rytov[13]: by matching Maxwell's boundary conditions inside the periodic structure, one can derive the indices for a wave propagating along the slits for each polarization state.

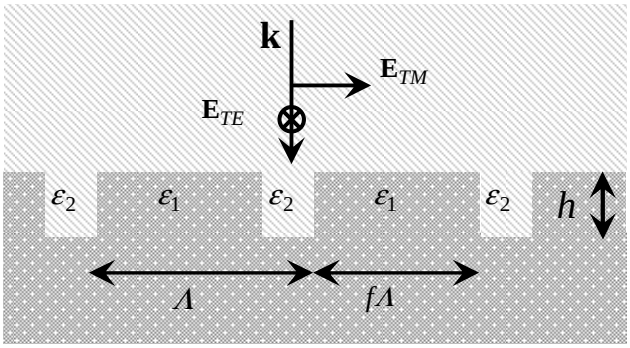

Fig. 3. Cross-view of a subwavelength grating. f is the fill factor, $f\,\Lambda$ represents the wall width, and $(1-f)\Lambda$ is the slit width.

In fact, Rytov provides transcendental equations that lead to an analytical solution for the TE polarization, but a Taylor expansion is necessary to extract a solution for the TM mode. Lalanne and Lemercier-Lalanne[14] used the Fourier expansion method first developed by Bell *et al.*[15] to extract general expressions for both effective indices. If Λ is the grating mini-period (Fig. 3), the second-order approximations, as a function of the ratio Λ/λ, write :

$$n_{TE} = \sqrt{f\,\varepsilon_1 + (1-f)\varepsilon_2}\,\sqrt{1 + \frac{1}{f\,\varepsilon_1 + (1-f)\varepsilon_2}\left(\frac{\Lambda}{\lambda}\right)^2 \sum_{r\neq 0} \frac{\varepsilon^{-r}\,\varepsilon^{r}}{r^2}} \tag{1}$$

$$n_{TM} = \sqrt{\frac{\varepsilon_1\,\varepsilon_2}{f\,\varepsilon_2 + (1-f)\varepsilon_1}}\,\sqrt{1 + \left(\frac{\varepsilon_1\,\varepsilon_2}{f\,\varepsilon_2 + (1-f)\varepsilon_1}\right)^2 \left(\frac{\Lambda}{\lambda}\right)^2 \sum_{r\neq 0}\sum_{m\neq 0} \frac{a^{-r}\,a^{m}\,\varepsilon^{r-m}}{m\,r}} \tag{2}$$

where f is the fill-factor so that $f\Lambda$ represents the fraction of the mini-period filled with material of relative permittivity ε_1 and $(1-f)\Lambda$ the fraction filled with material of relative permittivity ε_2, λ is the wavelength of light in vacuum, ε^q are the Fourier coefficients of the relative permittivity $\varepsilon(x)$ of the Λ-periodic structure, so that:

$$\varepsilon(x) = \sum_q \varepsilon^q\, e^{i\frac{2\pi}{\Lambda} q\, x} \tag{3}$$

#9238 - $15.00 USD Received 25 October 2005; revised 18 November 2005; accepted 21 November 2005

Similarly, a^q are the Fourier coefficients of the inverse $1/\varepsilon(x)$. These effective index formulas are believed to be valid for any dielectric structure, be they symmetric or not. In the case of symmetric structures explored in this paper, they simply reduce to:

$$n_{TE} = \sqrt{f\,\varepsilon_1 + (1-f)\varepsilon_2}\ \sqrt{1+\frac{\pi^2}{3}\left(f\,\varepsilon_1+(1-f)\varepsilon_2\right)\left(\frac{f(1-f)\Lambda}{\lambda}\right)^2\left(\frac{\varepsilon_1-\varepsilon_2}{f\,\varepsilon_1+(1-f)\varepsilon_2}\right)^2} \quad (4)$$

$$n_{TM} = \sqrt{\frac{\varepsilon_1\varepsilon_2}{f\,\varepsilon_2+(1-f)\varepsilon_1}}\ \sqrt{1+\frac{\pi^2}{3}\left(f\,\varepsilon_1+(1-f)\varepsilon_2\right)\left(\frac{f(1-f)\Lambda}{\lambda}\right)^2\left(\frac{\varepsilon_1-\varepsilon_2}{f\,\varepsilon_2+(1-f)\varepsilon_1}\right)^2} \quad (5)$$

which are similar to those obtained by Brauer and Bryngdahl[16], who derived their formulas from Rytov's transcendental equations. The first square root in each formula represents the first order approximation of the effective optical index. The second square roots in the expressions are symmetric and integrate the second-order correction.

The EMT approach appears to be quite adequate for a quick and intuitive study. As to its validity, it was carefully studied, confirmed and quantified by several authors. Some precautions are however necessary.

First, as was noted by Pommet *et al.*[17], the effective properties of subwavelength gratings cannot be simply described by an effective index, in particular when the grating thickness h is much smaller than the wavelength ($h << \lambda$). In that limit case, an effective thickness has to be introduced to accurately describe the effective properties. In order to preserve the simplicity of our approach, and following the conclusions of Ref. [18], we will thus explore situations for which $h \geq \lambda/3$.

Second, the grating mini-period Λ must obey both limitations[19] $\Lambda << \lambda$ (condition for the EMT approach) and $\Lambda \leq \lambda/n$ (condition for a zero-order diffraction scheme) where n is the index of the grating substrate, i.e., $n^2 = \varepsilon_1$ in the structure of Fig. 3. In the case of a high index substrate, we choose $\Lambda = \lambda/2n$, which automatically satisfies both conditions. Besides, the use of the complete second-order formulas (in terms of Λ/λ) is a guarantee to stay within acceptable approximations for the EMT approach. Indeed, Lalanne and Lemercier-Lalanne[14] showed that the 2nd order approximation remains within a good agreement with the rigorous coupled-wave analysis (RCWA) computations providing that $\Lambda/\lambda < 0.25$ for the TE case, and even for $\Lambda/\lambda < 0.4$ for the TM case.

Finally, there is a last condition on the grating period p, which must be much larger than the wavelength ($p >> \lambda/n$), in order to obtain a macroscopic diffraction effect.

From Eq. (4) and Eq. (5), it is easy to see that any effective optical index profile can be coded by tuning the fill factors f. This propriety will be used to code the WPD, as shown in Section 3.

3. A WPD structure on gallium arsenide

Gallium arsenide (GaAs) is a major infrared material with a very low absorption coefficient, in the order of $5.10^{-4}\,cm^{-1}$ from $\lambda = 1\mu m$ to $\lambda = 20\mu m$. It is besides a semiconductor of the technological mainstream, which means that it benefits from mature technology for growth, etching, polishing, deposition, etc… and that its material properties (both electronic and

#9238 - $15.00 USD Received 25 October 2005; revised 18 November 2005; accepted 21 November 2005

optical) are well-known. We base our study on the optical index calculated with the Sellmeier coefficients provided by Adashi[20].

$$n_{GaAs}(En) = \sqrt{7.1 + \frac{3.78}{1 - 0.180\,En^2} - \frac{1.97}{(30.08\,En)^2 - 1}} \qquad (6)$$

where $En = 1.24/\lambda$ is the energy of a photon in electron-Volt if λ is the wavelength in micrometers. This formula stands for the spectral range from $1\mu m$ to $20\mu m$.

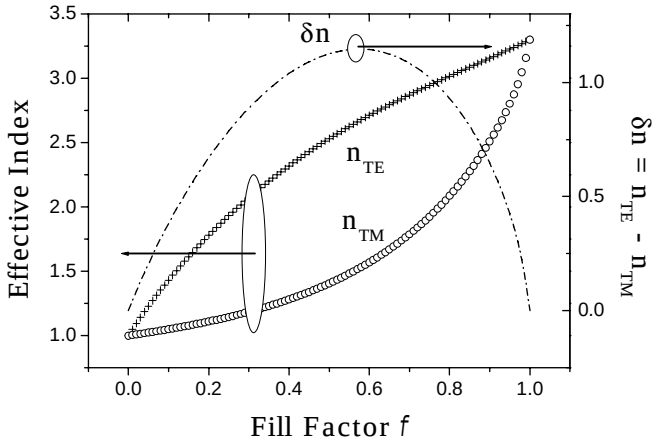

Fig. 4. Effective index of subwavelength gratings on a GaAs substrate as a function of the fill-factor f. We also draw the induced birefringence $\delta n = n_{TE} - n_{TM}$ ($\lambda = 5\mu m$ and $\Lambda = \lambda/2n_{GaAs}$)

We consider a grating etched in a GaAs wafer totally immersed in air ($n_{air} = 1$). A normal incidence is supposed. Figure 4 shows the variations of the effective index for both polarization states TE and TM as a function of the fill factor f, for a wavelength value $\lambda = 5\mu m$ and $\Lambda = \lambda/2n_{GaAs}$. As is illustrated on Fig. 4, the structure is highly birefringent ($\delta n = n_{TE} - n_{TM}$ can be higher than 1, in the case of a GaAs grating). This is due to the high index difference between the two dielectrics composing the grating ($n_{air} = 1$ and $n_{GaAs} \approx 3.3$). One should point out that such an index gap is necessary to code a blazed grating. Otherwise, a great thickness h is needed to allow the phase variation between 0 and 2π on each sub-period, as well as subwavelength structures Λ, the combination of which may be beyond the possibilities of actual etching processes. From that point of view, the high optical index of GaAs is a major point for the WPD applications. One could also imagine using even higher optical index materials, such as germanium (Ge)…

#9238 - $15.00 USD Received 25 October 2005; revised 18 November 2005; accepted 21 November 2005

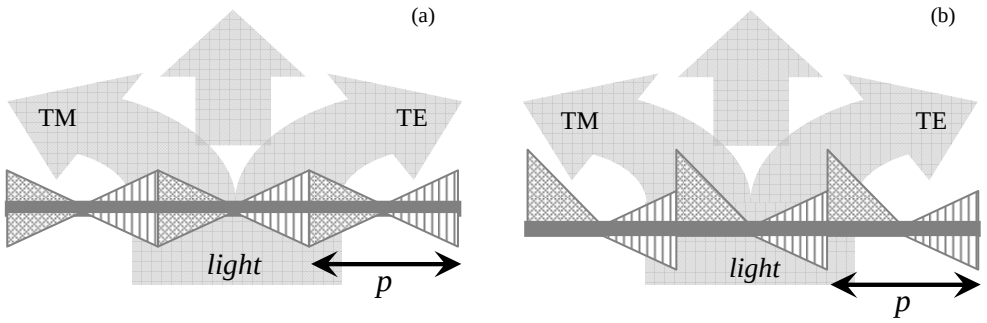

Fig. 5. WPD geometries : (a) the phaseshift is coded between 0 and π on each side of the plate, for both the TE and TM polarization state; (b) the phaseshift is coded between 0 and 2π on one side for TM and between 0 and π on each side for the TE state.

The idea is to code a triangular optical index variation on each period, in order to get a linear variation of the phase φ from 0 to 2π for the TE state on the one sub-period of dimension $p/2$ (whereas the phase for TM remains constant), and from 2π to 0 for the TM state on the next sub-period of same dimension $p/2$ (whereas the phase for TE remains constant). It must be pointed out, however, that one can not act on one polarization state and leave the other one unchanged: each action on the TE (resp., TM) wave will have an influence on the TM (resp., TE) polarization. We thus explored two typical geometries. The first is a one-sided grating, with a linear variation of the phase between 0 and 2π as illustrated on Fig. 1. The second geometry is a two-sided grating, with various scenarios of phase variations on each side of the plate, be they linear or non linear (Fig. 5). One can for instance imagine structures where a convex phase variation on one side of the substrate combines to a concave variation on the other side to get a globally linear phase coding on each period of the grating ; unfortunately, calculations show that this kind of structure does not prove efficient.

#9238 - $15.00 USD Received 25 October 2005; revised 18 November 2005; accepted 21 November 2005

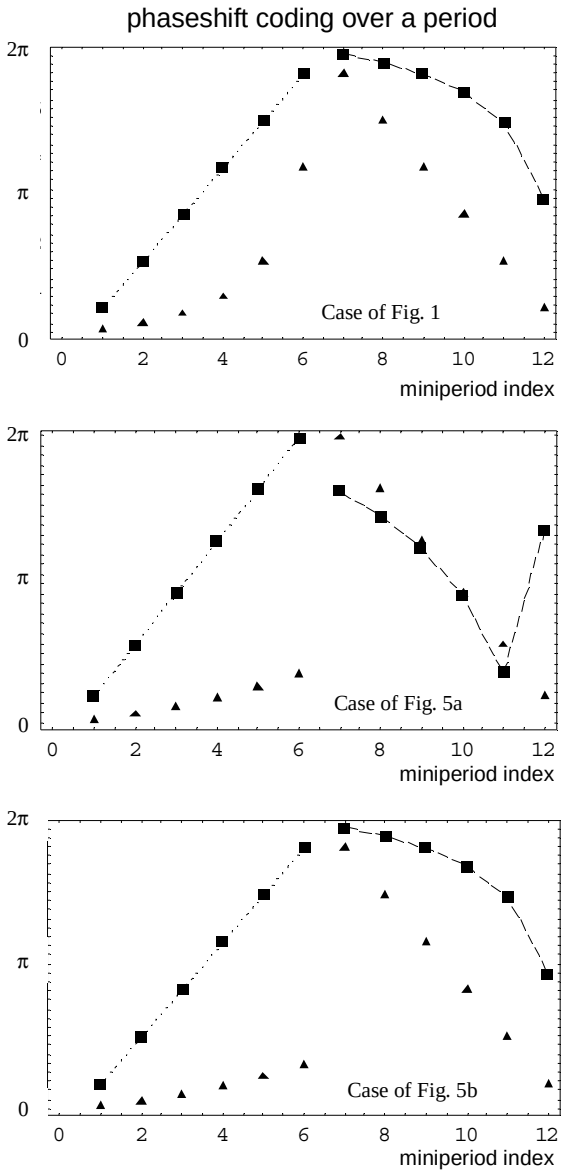

Fig. 6. Phaseshift coding by various binary subwavelength grating geometries (scatter triangle: TM, joined box: TE). Each period is devided into 12 miniperiods. The case of Fig. 5(a) is a poor approximation of the desired geometry, since both TE and TM polarizations undergo the same phaseshift on the second half of the period. The case of Fig. 5(b) is similar to the case of Fig. 1, except that it provides a better approximation for the TM polarization on the first half of the period.

Each geometry is then tested in term of phaseshift coding (Fig. 6). This criteria helps to find out which geometries are adapted. There clearly appears that the structure of Fig. 1 provides a fair approximation, and that the structure of Fig. 5(b) is the most suited to a WPD application. This last structure however requires a carefully designed thickness of the plate. Indeed, the upper and lower diffraction patterns could otherwise be mis-aligned, as is illutrated in Fig. 7.

#9238 - $15.00 USD Received 25 October 2005; revised 18 November 2005; accepted 21 November 2005

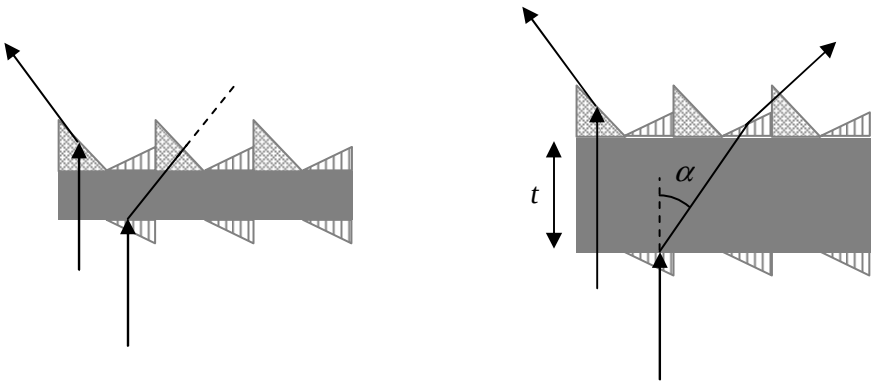

Fig. 7. In case of a mis-calculated thickness of the substrate, the upper and lower diffraction patterns could be mis-aligned.

In that case, the important feature is the refraction angle α inside the plate. A straightforward calculation shows that a substrate thickness of $t = j * 30\mu$m, j an integer, would allow a correct superposition of the upper and lower diffracted waves. For instance, a typical thickness of 300μm could be chosen.

Then, the geometries are studied in term of diffraction efficiency (Fig. 8). In order to evaluate the diffraction efficiency, the WPD is assumed to be a thin grating described by a transmittance $t_\theta(x) = \exp(i\varphi_\theta(x))$ of period Λ, for the θ-polarized wave. The transmittance may be written as a Fourier series:

$$t_\theta(x) = \sum_v c_{v,\theta} \exp\left(iv \frac{2\pi}{\Lambda} x \right) \tag{7}$$

$c_{v,\theta}$ being the Fourier coefficients of the grating transmittance. The intensity of the v^{th} order diffracted for the θ-polarized wave is then weighed by $\left| c_{v,\theta}^2 \right|$. It is noteworthy that the v^{th} order diffracted TE wave is collinear to the $(-v)^{\text{th}}$ order diffracted TM wave in the explored grating geometries.

The important feature is the extinction ratio, which corresponds to the ratio of parasitic light over the useful diffracted light in the same direction. If one considers the TE-polarized v^{th} order diffracted wave, the extinction ratio thus writes:

$$ER_{TE} = \left| \frac{c_{-v,TM}}{c_{v,TE}} \right|^2 \tag{8}$$

A similar expression is derived for ER_{TM}.

As can be expected, the unilateral geometry of Fig. 1 provides a symmetric diffraction pattern, which appears to be quite different from the mixed geometry of Fig. 5b. It is noteworthy that these structures do not annihilate the 0^{th} diffracted order. But fortunately this parasitic order keeps a small weight, which is a major point for Wollaston prism conception. One can however decide, in order to get rid of the 0^{th} order, to study the geometry of Fig. 9 : it uses a super-imposed odd grating, coding phase lags of alternatively 0 and π radians for both polarisation states. This is obtained by simply modulating the thickness of the substrate.

#9238 - $15.00 USD Received 25 October 2005; revised 18 November 2005; accepted 21 November 2005

Eventually, both criterias (phaseshift coding and diffraction criteria) undoubtedly show that the geometry of Fig. 5b is best suited to the WPD application. This geometry is expected to reach an extinction ratio of 30% and 10% on the second diffracted orders ($+2TM$ and $+2TE$). And the geometry of Fig. 9 proves even more efficient if the third orders of diffraction are considered ($+3TM$ and $+3TE$), which then provides an extinction ratio as low as 14% or 2%.

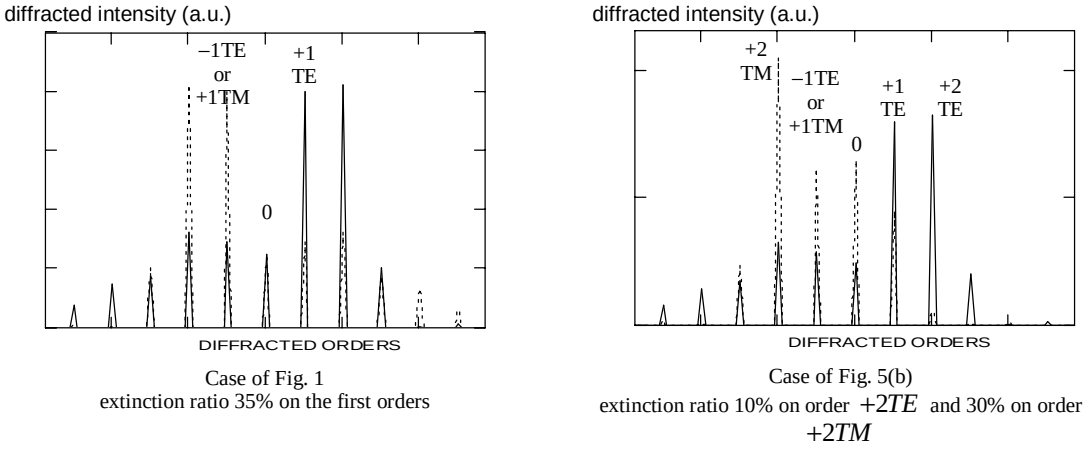

Case of Fig. 1
extinction ratio 35% on the first orders

Case of Fig. 5(b)
extinction ratio 10% on order $+2TE$ and 30% on order $+2TM$

Fig. 8. Diffraction pattern of various binary subwavelength grating geometries (TM : dashed lines; TE : straight lines). The extinction ratio is evaluated with the two first useful orders in each case (see rectangular boxes).

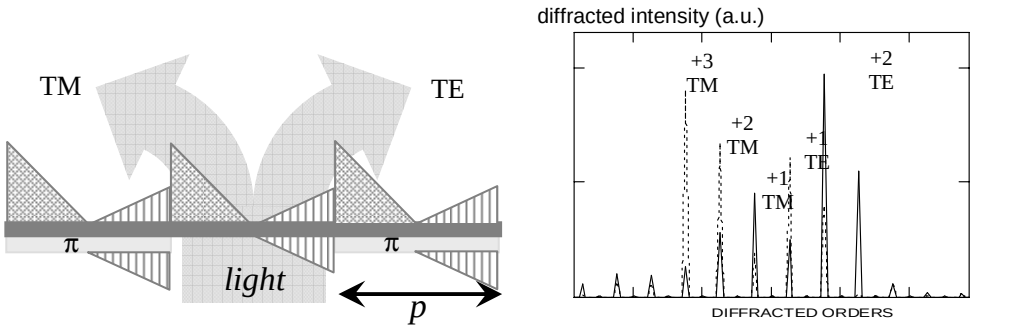

extinction ratio 2% on order $+3TE$ and 14% on order $+3TM$

Fig. 9. Optimized WPD geometry based on Fig. 5(b). The phaseshift is coded between 0 and 2π on one side for TM and between 0 and π on each side for the TE state. A supplementary phaseshift of π is periodically added, in order to annihilate the 0^{th} transmitted order.

4. Spectral performances of the GaAs-based WPD

For an illustration purpose, let us describe the particular case of Fig. 5(b): the phaseshift is coded between 0 and 2π on one side of the plate for the TM state, and between 0 and π on both sides of the plate for the TE state.

#9238 - $15.00 USD Received 25 October 2005; revised 18 November 2005; accepted 21 November 2005

The optimal thickness of the grating is chosen to be $h = \lambda/(n_{GaAs} - n_{air})$ in order to allow a maximum phase shift of 2π. For an illustration purpose, we choose $\lambda = 5\mu m$ and $h = 2.17\mu m$. We choose the same height h for all the gratings, since this is the most technologically sound geometry. The optical effective index (and subsequently the phaseshift) coding is obtained through the fill factor. The mini-period is then fixed to $\Lambda = \lambda/(2\,n_{GaAs}) = 0.76\mu m$ (see section II for respect of the EMT approach limitations in terms of h and Λ).

Let us now calculate the values of the fill factor f which allow a linear variation of the phase on a sub-period $p/2$. Each sub-period is divided into nb parts or mini-periods of dimension Λ. Within each period , the u^{th} mini-period ($u \in [1, nb]$) will ideally code a phase $\varphi_u{}^{TE} = \pi \dfrac{u - 0.5}{nb}$ for the TE state and a zero-phase for TM. Whereas the u^{th} mini-period ($u \in [nb+1,\ 2nb]$) will ideally code a phase $\varphi_u{}^{TM} = 2\pi\left(1 - \dfrac{u - nb - 0.5}{nb}\right)$ for the TM state, and a zero-phase for TE. By reversing the Bauer and Brynghdal formulas providing n_{TE} and n_{TM}, one can get the corresponding values of $f_u{}^{TE}$ and $f_u{}^{TM}$. Following the case of Fig. 6, we choose $nb = 6$.

Table 1. (a) The grating follows the geometry of Fig. 5b. These are the computed values for the TE State ($\lambda = 5\mu m$, $h = 2.17\mu m$, $\Lambda = 0.76\mu m$).

		Wall width	Slit width
# of mini-period	$f_u{}^{TE}$	$f_u{}^{TE}\Lambda$ (nm)	$(1 - f_u{}^{TE})\Lambda$ (nm)
1	0	0	760
2	0.07	**50**	710
3	0.11	**80**	680
4	0.17	**130**	630
5	0.23	**180**	580
6	0.30	**230**	530

Table 1. (b) The grating follows the geometry of Fig. 5b. These are the computed values for the TM State ($\lambda = 5\mu m$, $h = 2.17\mu m$, $\Lambda = 0.76\mu m$).

		Wall width	Slit width
# of mini-period	$f_u{}^{TM}$	$f_u{}^{TM}\Lambda$ (nm)	$(1 - f_u{}^{TM})\Lambda$ (nm)
7	0.99	0	760
8	0.94	**50**	710
9	0.86	**100**	660
10	0.76	**200**	560
11	0.60	**300**	460
12	0.31	500	**260**

#9238 - $15.00 USD Received 25 October 2005; revised 18 November 2005; accepted 21 November 2005

Table 1 summarizes the results in the case where $nb = 6$ mini-periods. The grating period is then $p = 9\mu m$, thus much higher than the wavelength. The same theoretical study is made for the grating of Fig. 1, and the main features are summarized on Table 2.

Table 2. The grating follows the geometry of Fig. 1. These are the computed values for the TE State ($\lambda = 5\mu m$, $h = 2.17\mu m$, $\Lambda = 0.76\mu m$). The values for the TM state are the same as in Table 1(b).

		Wall width	Slit width
# of mini-period	f_u^{TE}	$f_u^{TE}\Lambda$ (nm)	$\left(1 - f_u^{TE}\right)\Lambda$ (nm)
1	0	0	760
2	0.14	**100**	660
3	0.26	**200**	560
4	0.41	**360**	400
5	0.61	460	**300**
6	0.87	660	**100**

On both tables, the important technological values (i.e., limiting technological features) are written in bold characters within greyed cells, being in some cases the wall widths and in the other cases the slit widths. These values correspond to state-of-the-art etching capabilities. Indeed, to estimate the feasibility of the proposed concept, fabrication constraints should be taken into account. The fabrication procedure should provide accurate control over the duty ratio and the grating profile, uniform etching depth, smooth surfaces, and high aspect ratios. Several authors[21-23] demonstrated the fabrication of such high-quality structures with features on the 100-nm scale. For instance, appreciably regular slits wide of $90nm$ and high of $3\mu m$ have been achieved by the CNRS/LPN in France[21], which thus ensures the feasibility of such WPD structures.

It is eventually noteworthy that the subwavelength structures can be designed for broadband illumination[24]. The WPD described in section III could be generalized to other wavelength ranges, for instance in the Band III spectral region, or more precisely for CO_2 laser applications.

Let us now quantify the spectral behaviour of a 5µm-designed WPD. Figure 10 shows the phaseshift variations in the structure for various wavelengths λ. This is an illustration in the case of Fig. 1. As is easily predictable since the optical index of both air and GaAs are very low dispersive in this spectral range, the linear variation of the phaseshift is conserved. However, the phaseshift borders vary noticeably within the 0 and 2π limits.

#9238 - $15.00 USD Received 25 October 2005; revised 18 November 2005; accepted 21 November 2005

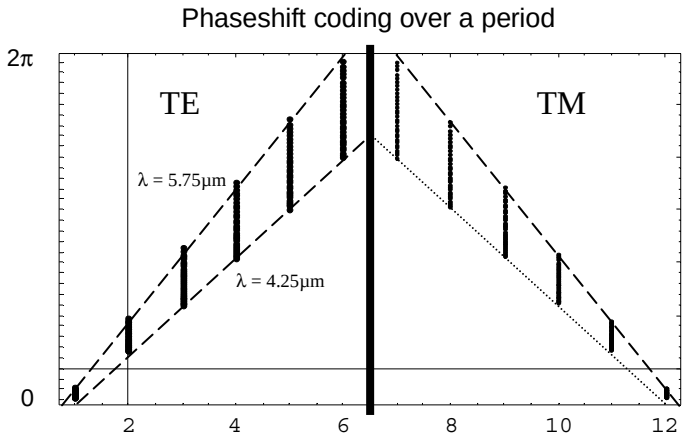

Fig. 10. Phaseshift introduced by a 5µm-designed WPD in the 4.25µm-5.75µm range within each period. This illustrates that the WPD is naturally spectrally broadband.

Figure 10 shows that the 5µm-designed WPD admits a spectral bandwidth covering at least the region from $\lambda = 4.25\mu m$ to $\lambda = 5.75\mu m$, thus proving spectrally broadband. Besides, if one considers the satisfying case of Fig. 5(b), the calculations show that the extinction ratio remains better than 35% within these wavelength limits.

5. Conclusion

Continuous progress of etching techniques allow to imagine, conceive and realize more and more compact structures made of subwavelength-scale optical elements. We present and analyze a novel concept of Wollaston-prism like device, for an application in the infrared range. It uses the concept of graded-index coding by subwavelength structures. The proposed geometry is based on etching a 1-D periodic subwavelength structure with a varying duty cycle. Alternate linear variations of the index for both polarizations are achieved by modifying the duty cycle of the structure gradually along one axis of the substrate, while the period is kept constant. This allows to code linear variations of the phaseshift, in order to satisfy blazing conditions for TE and TM waves. The designed structure thus diffracts cross-polarized light rays in symmetric directions. This optical tool could answer various needs, from the near to the far-infrared spectral range. Besides, on the basis of tolerance analysis, we believe that the realization of these novel devices is achievable with current fabrication technology.

#9238 - $15.00 USD Received 25 October 2005; revised 18 November 2005; accepted 21 November 2005